Mutations affecting development of the notochord in zebrafish

Derek L. Stemple*, Lilianna Solnica-Krezel*, Fried Zwartkruis[1], Stephan C. F. Neuhauss, Alexander F. Schier[2], Jarema Malicki, Didier Y. R. Stainier[3], Salim Abdelilah, Zehava Rangini[4], Elizabeth Mountcastle-Shah and Wolfgang Driever[†]

Cardiovascular Research Center, Massachusetts General Hospital and Harvard Medical School, 149 13th Street, 4th Floor, Charlestown, MA 02129, USA

*Contributed equally to the work
[1]Present address: Laboratory for Physiological Chemistry, Utrecht University, 3584 CG Utrecht, The Netherlands
[2]Present address: Skirball Institute of Biomolecular Medicine, New York University Medical Center, 550 First Avenue, New York, NY 10016, USA
[3]Present address: Department of Biochemistry and Biophysics, University of California San Francisco, San Francisco, CA 94143-0554, USA
[4]Present address: Department of Oncology, Sharett Institute, Hadassah Hospital, Jerusalem 91120, Israel
[†]Author for correspondence (e-mail: driever@helix.mgh.harvard.edu)

SUMMARY

The notochord is critical for the normal development of vertebrate embryos. It serves both as the major skeletal element of the embryo and as a signaling source for the establishment of pattern within the neurectoderm, the paraxial mesoderm and other tissues. In a large-scale systematic screen of mutations affecting embryogenesis in zebrafish we identified 65 mutations that fall into 29 complementation groups, each leading to a defect in the formation and/or maintenance of the notochord. These mutations produce phenotypic abnormalities at numerous stages of notochord development, thereby establishing a phenotypic pathway, which in turn suggests a genetic pathway for the development of the notochord. Perturbations within adjacent tissues in mutant embryos further indicate the importance of notochord-derived signals for patterning within the embryo and suggest that these mutations will yield additional insight into the cues that regulate these patterning processes.

Key words: zebrafish, notochord, floor plate, mesoderm, embryogenesis

INTRODUCTION

The notochord is a structure common to all members of the phylum Chordata. It serves as the major skeletal element for lower chordates and as such provides an important mechanical element for the locomotion of the individual. In lower vertebrates at larval stages of development the notochord plays a similar role serving as the major skeletal element in the body apparently necessary for coordinated movement. Perhaps more importantly, in all vertebrates, the notochord is required for the proper patterning of adjacent tissues, including the neurectoderm, paraxial mesoderm and the heart. In the neurectoderm, the notochord functions to signal the formation of the floor plate, and, independently, can signal the formation of motoneurons (Placzek et al., 1993; van Straaten et al., 1988; Yamada et al., 1993). In addition to specifying ventral fates the notochord suppresses the expression of dorsal fates in the neurectoderm (Bovolenta and Dodd, 1991; Goulding et al., 1993). The notochord appears to play several roles in the patterning of somitic tissue. First, based on experimental manipulation of avians as well as analysis of several mouse mutations, the notochord is responsible for the specification and maintenance of ventral, i.e. sclerotome, fates in the somite (Dietrich et al., 1993; Pourquie et al., 1993). The notochord is also involved in dermomyotome patterning. In avian experiments, notochord extirpation leads to a complete loss of epaxial muscles, i.e. deep back muscles, whereas hypaxial muscles, i.e. limb and ventrolateral body wall muscles, are unaffected (Christ et al., 1992; Rong et al., 1992). Muscle specification occurs in the absence of notochord, but a notochord derived signal is required to maintain the epaxial muscle fate (Bober et al., 1994). Mosaic analysis of the zebrafish mutation *no tail* (*ntl*), a mutation in a gene homologous to the mouse *Brachyury* gene, indicates that differentiated notochord is also required for the proper patterning of muscle pioneers in the developing myotome (Halpern et al., 1993; Herrmann et al., 1990; Schulte-Merker et al., 1992). Interestingly, mutants of the *ntl* locus form a floor plate (Halpern et al., 1993), suggesting that not all of the notochord signaling activities are disrupted by the mutation. In addition to its role in patterning the CNS and somites, the notochord may also serve to specify other tissues such as sympathoadrenal progenitors (Stern et al., 1991), the left-right asymmetry of the heart tube (Danos and Yost, 1995), and the differentiation of certain gut derivatives (Wiertz-Hoessels et al., 1987). There is evidence that specification of the floor plate and patterning of the somite are both mediated at least in part by *Sonic hedgehog* (*shh*) (Fan et al., 1995; Fan and Tessier-Lavigne, 1994;

Johnson et al., 1994a; Roelink et al., 1994). Other peptide growth factors, such as bone morphogenic proteins BMP-2 and BMP-7 have also been found to be expressed in the notochord (Lyons et al., 1995). Taken together these data point to the importance of the notochord, not only for the structural integrity and locomotion of the embryo, but also for the establishment of axial pattern within the mesoderm, neurectoderm and other tissues. Additional mutations affecting notochord development would therefore provide insight into the mechanisms governing notochord differentiation, the tissue interactions underlying the establishment of axial patterning, and ultimately, to the molecular determinants mediating these events.

The entire axial mesoderm, that is the prechordal plate and the notochord are derived from the dorsal organizer. The organizer was originally identified by its ability to induce the ectopic formation of dorsal-anterior structures when transplanted into embryonic regions that would otherwise give rise only to more ventral and lateral structures (Spemann, 1938). The organizer, originally described for amphibia, is functionally equivalent to the embryonic shield of teleost fish (Ho, 1992; Oppenheimer, 1936). In normal development the organizer provides an activity primarily responsible for the induction of the axis of the embryo. Importantly, transplanted organizer will cause host tissue to acquire novel fate while contributing predominantly to the prechordal plate, notochord and partially to somites and neurectoderm.

Morphologically distinguishable stages are apparent during notochord development in zebrafish (Kimmel et al., 1995). Soon after the onset of the gastrulation movements, the direct antecedent of the notochord, the chordamesoderm, can be distinguished from the paraxial mesoderm by virtue of its continued expression of the *Brachyury* gene (Herrmann et al., 1990; Schulte-Merker et al., 1992) and by the expression of a number of other molecular markers including *Shh*, and later *α1-collagen Type II* (*col2a1*) (Yan et al., 1995). Prior to segmentation the chordamesoderm becomes morphologically distinct from the paraxial mesoderm. During the segmentation period of development, central cells of the notochord differentiate and acquire a large vacuole. The entire notochord becomes surrounded by a sheath of tissue, which in combination with the turgor pressure generated by the vacuolated cells imparts to the notochord its stiffness (Adams et al., 1990). As notochord cells become vacuolated, the expression of *Brachyury, shh* and *col2a1* are each extinguished in the notochord (Schulte-Merker et al., 1992). Expression of *shh* is maintained in the floor plate and *col2a1* continues to be expressed both in the floor plate and the hypochord (Krauss et al., 1993; Yan et al., 1995).

The *Brachyury* gene was originally identified by mutation and was ultimately cloned by virtue of a number of mutations including a key insertion (Herrmann et al., 1990). The gene encodes a nuclear factor that appears to control the formation of caudal segments of the organism as well as the differentiation of the notochord. Apart from *Brachyury*, available mouse mutations affecting the notochord are: *Danforth's short-tail* (*Sd*), which results in the loss of notochord at midgestation (Bovolenta and Dodd, 1991; Dietrich et al., 1993; Paavola et al., 1980; Phelps and Dressler, 1993); *Pintail* (*Pt*), in which reduction of the notochord size is a result of reduced mitotic rates (Berry, 1960); and *truncate* (*tc*) which causes interruptions and premature truncations in the notochord

(Theiler, 1959). In addition, several targeted gene disruptions, such as in the HNF-3β gene (Ang and Rossant, 1994; Weinstein et al., 1994), or in the fibronectin gene (George et al., 1993) produce notochord phenotypes in homozygous mutant mice.

In order to identify genes necessary for normal embryogenesis of vertebrates we have performed a systematic large-scale genetic screen. The details of the screen are described elsewhere (Driever et al., 1996). In this report the isolation and the genetic and phenotypic analysis of mutations affecting the formation and maintenance of the notochord are described. These mutations provide a genetic framework for dissecting the process of notochord specification and differentiation as well as further defining the role of the notochord in the development of other embryonic tissues.

MATERIALS AND METHODS

Animals

Fish were maintained in the zebrafish facility at the Cardiovascular Research Center, of Massachusetts General Hospital (Driever et al., 1996; Solnica-Krezel et al., 1994). Heterozygous stocks were generated by mating the originally identified heterozygous F_2 fish with wild-type AB strain (Johnson et al., 1994b), Hong-Kong strain, India strain (Knapik, 1996), or Tü strain (Mullins and Nüsslein-Volhard, 1993) partners; growing the outcrossed lines, then reidentifying heterozygous fish by sibling matings. Mutant and wild-type siblings for analysis were obtained by mating a male and female heterozygous for the given mutation. Embryos were raised at a constant 28°C and approximate stages are given in hours postfertilization at 28°C (hpf). Once a fish was identified as a heterozygous carrier it was crossed again for confirmation before being added to a pool of heterozygous fish. Four or more fish of a given genotype were maintained in 5 liter tanks as a pool of no more than 30 adult fish. Single fish were maintained in 1 liter boxes. All fish were raised and maintained as described by Solnica-Krezel et al. (1994).

Complementation testing

Allelism was tested first between mutations producing similar phenotypes. This defined a smaller number of complementation groups between which complementation tests were subsequently performed. For each complementation test an identified, confirmed heterozygous fish of one genotype was crossed with an identified, confirmed heterozygous partner of another genotype. For each complementation test a minimum of 30 embryos from a cross or group of crosses was examined. The embryos were scored on the days that the expected phenotypes normally appeared and at 5 days postfertilization (dpf) for
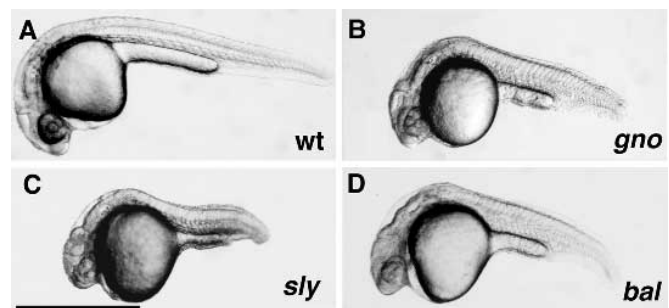

Fig. 1. Notochord differentiation mutants at 24 hpf. Micrographs of a 24 hpf wild-type (A) embryo and 24 hpf mutant embryos of the gno^{m622} (B), sly^{m86} (C), and bal^{m190} (D) loci. Scale bar, 1 mm.

the existence of an inflated swim bladder, which in the absence of any other phenotype indicates normal wild-type development. A pair of alleles are considered to be non-complementing (i.e. belonging to the same complementation group) when ~25% of the progeny of the cross were found to display the mutant phenotype. A total of 500 successful crosses were performed to determine the complementation groups, and a total of 42,628 embryos were scored giving an average of 85 embryos scored per complementation test. For each mutation tested, the identified heterozygous carriers were reidentified from outcrossed lines. Hence, fish used in the complementation testing or for molecular analysis were of generation F_3 or later.

In situ hybridization

In situ hybridization reactions were carried out essentially as described by Jowett and Lettice (1994); Oxtoby and Jowett (1993). Plasmid template cDNA for *Sonic hedgehog* was obtained from P. Ingham (Krauss et al., 1993); *α1-collagen Type II (col2a1)* from J. Postlethwait (Yan et al., 1995); and *Zf-T Brachyury* from S. Schulte-Merker (Schulte-Merker et al., 1992).

Immunohistochemistry

Embryos were fixed in a solution of 4% paraformaldehyde in PBS overnight at 4°C. Embryos were rinsed 3× in PBT (1× PBS, 0.1% Tween-20), then incubated in blocking solution (PBT, 2mg/ml BSA, 5% goat serum, 1% DMSO) for 1 hour and finally incubated overnight in a 1:1 mixture of blocking solution and hybridoma supernatant. Embryos were rinsed 4× with PBT over a 2 hour period then incubated overnight in blocking solution with 1:500 biotinylated goat anti-mouse (Vector Laboratories, Burlingame, CA). Embryos were rinsed 4× with PBT, then incubated for 2 hours at room temperature with Vectastain Elite ABC reagent (Vector Laboratories, Burlingame, CA) diluted 1:10 from the manufacturers recommendation in PBT.
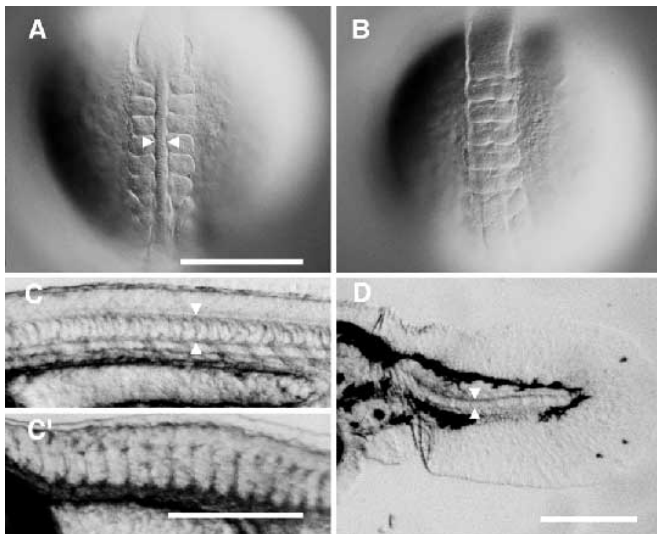
Embryos were rinsed 4× with PBT, then twice with acetate-imidazole buffer (175 mM sodium acetate, 10 mM imidazole, 0.1% Tween 20 in H_2O, pH 7.2). Embryos were then incubated for approximately 5 minutes in chromagen solution (125 mM sodium acetate, 10 mM imidazole, 100 mM Ni(II)SO_4·$6H_2O$, 0.3 mg/ml diaminobenzidine, 0.01% H_2O_2, and 0.1% Tween 20 in H_2O, pH 7.2) while being monitored under a dissecting microscope. The chromagen reaction was stopped by extensive rinsing with PBT. Monoclonal anti-Engrailed antibody producing hybridoma cells, 4D9, were obtained from the American Type Culture Collection (Hatta et al., 1991a).

RESULTS

A large-scale systematic screen for recessive-zygotic mutations affecting embryogenesis in zebrafish was carried out and has been described elsewhere (Driever et al., 1996; Solnica-Krezel et al., 1994). Among mutations affecting embryogenesis, approximately 10% display specific defects in the notochord. Most of the mutations affecting the notochord were identified at 1 dpf of screening. Several mutations, however, do not produce a phenotype until later in development and were identified during screening on 2, 3 or 5 dpf. Initial phenotypic analysis indicated that mutations affecting development of the notochord fall into several categories,
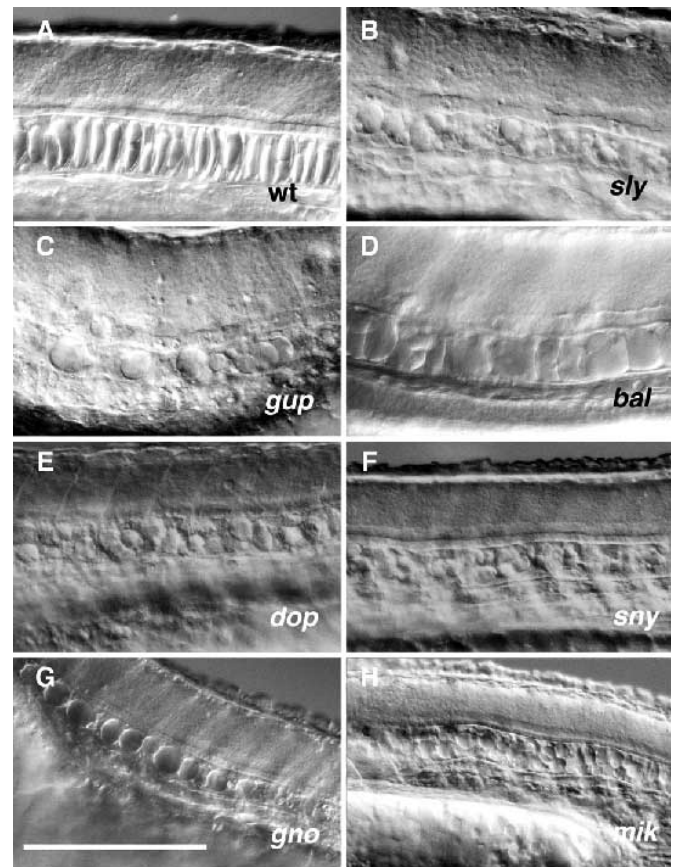

Fig. 2. Chordamesoderm and notochord phenotypes of *boz* mutants. DIC micrographs of a (A) wild-type (arrowheads indicate sides of the chordamesoderm) and (B) *boz* mutant embryo at the 10-somite stage demonstrate the absence of chordamesoderm in *boz^{m168}* mutant embryos. In (A) the chordamesoderm is shown bisecting the paired somites. The chordamesoderm is missing in the *boz^{m168}* mutant embryo (B) resulting in the lateral fusion of somites. (C,C′) At 24 hpf a vacuolated notochord normally seen in wild-type embryos (C; between arrowheads) is completely missing in the *boz* mutant embryo (C′). (D) Variable expressivity of the phenotype is observed as some *boz* mutant embryos form a notochord (between the arrowheads) in the tail as seen in this 72 hpf embryo tail. Scale bars, 250 μm.

Fig. 3. Notochord phenotype of mutants in the *sly*, *gup*, *bal*, *dop*, *sny*, *gno* and *mik* loci at 24 hpf. DIC micrographs of a 24 hpf (A) wild-type embryo, and 24 hpf (B) *sly^{m466}*, (C) *gup^{m189}*, (D) *bal^{m190}*, (E) *dop^{m341}*, (F) *sny^{m456}*, (G) *gno^{m622}*, and (H) *mik^{m218}* mutant embryos demonstrate the failure of mutant notochords to differentiate normally and form vacuolated cells. Scale bar, 250 μm.

according to stage of notochord development they affect: (1) chordamesoderm specification and/or maintenance (Group I); (2) notochord differentiation (Groups II-IV); and (3) notochord maintenance (Group V) (Table 1). Additionally, several mutations were found that affect the shape of the notochord.

Finally, several mutations with relatively mild effects on the notochord shape appear to affect the formation and/or maintenance of the floor plate or central canal of the spinal cord. Mutations affecting the floorplate were tested for allelism with the other notochord mutations and are included in the table but

Table 1. Complementation groups of mutations affecting notochord development

Locus name	Alleles	Category**	Phenotype	Other defects	Refs
Group I					
bozozok (boz)*	*m168*	A, B	No chordamesoderm	Reduced floor plate, cyclopia	a
floating head (flh)*	*m614*	B, C	No chordamesoderm	Reduced floor plate	b
Group II					
no tail (ntl)*	*m147, m550*	B, C	Notochord fails to vacuolate	Posterior segments not specified	c, d, e
gno (gno)	*m622*	B, C	Notochord fails to vacuolate		
Group III					
sleepy (sly)*	*m86, m91, m99, m152, m253, m388, m466, m515, m516, m707*	A, C	Notochord fails to vacuolate	Brain defects, eye defects	f
bashful (bal)*	*m102, m113, m190, m255, m268, m277, m290, m296, m430, m473, m373*	A, C	Notochord fails to vacuolate	Brain defects, eye defects	f
grumpy (gup)*	*m135, m189, m217, m726, m753*	A, C	Notochord fails to vacuolate	Brain defects, eye defects	f
Group IV					
dopey (dop)*	*m341, m475*	B, C	Notochord fails to vacuolate	d2 embryo degeneration	
sneezy (sny)*	*m456*	B, C	Notochord fails to vacuolate	d2 embryo degeneration	
mikry (mik)	*m218*	A, B, C	Notochord fails to vacuolate	d3 embryo degeneration	
nototod (not)	*m128*	B	d2 notochord degeneration	d2 somite degeneration	
Group V					
snow white (snw)	*m454*	B	d3 notochord shortened, d1 spherical notochord cells	Melanophores lightly pigmented	
changeling (chg)	*m275*	B	d2 spherical notochord cells	Not fully penetrant	
maggot (mgt)	*m350, m503, m635*	A, B, D	d1 spherical notochord cells, d2 notochord shorter	Head smaller, jaw/arch defects	
mind bomb (mib)	*m132, m178*	A, D	d1 sperical notochord cells, d2 notochord thinner	CNS neurogenesis defects	f
Group VI					
gitolo (git)	*m342*	B	d3 notochord shortened	Not fully penetrant	
drobny (drb)	*m759*	B	d3 notochord shortened	Viable	
snorri (sno)	*m563, m672*	B	d3 notochord shortened		
proteus (pro)	*m642*	B	Notochord breaks	Not fully penetrant	
Group VII					
gulliver (gul)	*m208*	A, B	d1 folded notochord	Head small	
leviathan (lev)	*m531*	B	Folded notochord	Partially dominant	
trilobite (tri)*	*m144, m209, m747, m778*	A, B	Notochord folded in tail	Slowed convergence	a
knypek (kny)	*m119*	A, B	Notochord folded in tail	Slowed convergence	a
heads up (hup)	*m438, m420, m568*	B, D	Notochord thinner	Head small, uncoordinated body movements	
Group VIII					
one-eyed pinhead (oep)*	*m134*	A	Notochord curved ventrally	d1 reduced floor plate, cyclopia	a, f
cyclops (cyc)*	*m101, m122, m294*	A	Persistent *col2a1* expression	d1 reduced floor plate, cyclopia	g, h
uncle freddy (unf)	*m768*	A	Notochord curved ventrally, breaks in sheath	Reduced floor plate d1, mild cyclopia	f
Group IX					
falisty (fal)	*m371*	A	Notochord curved	Reduced neurocoel	
falowany (flw)	*m735*	A	Notochord curved	Reduced neurocoel, ear malformations	

*Complementation testing has been preformed between these loci and the Tübingen group loci of the same name.

**Category: four different groups of loci (A, B, C, D) were tested for complementation. For example all loci listed as category A were mutually tested and constitute distinct complementation groups.

a, Solnica-Krezel et al. (1996); b, Talbot et al. (1995); c, Schulte-Merker et al. (1994); d, Schulte-Merker et al. (1992); e, Halpern (1993); f, Schier et al. (1996); g, Hatta et al. (1991b); h, Yan et al. (1995).
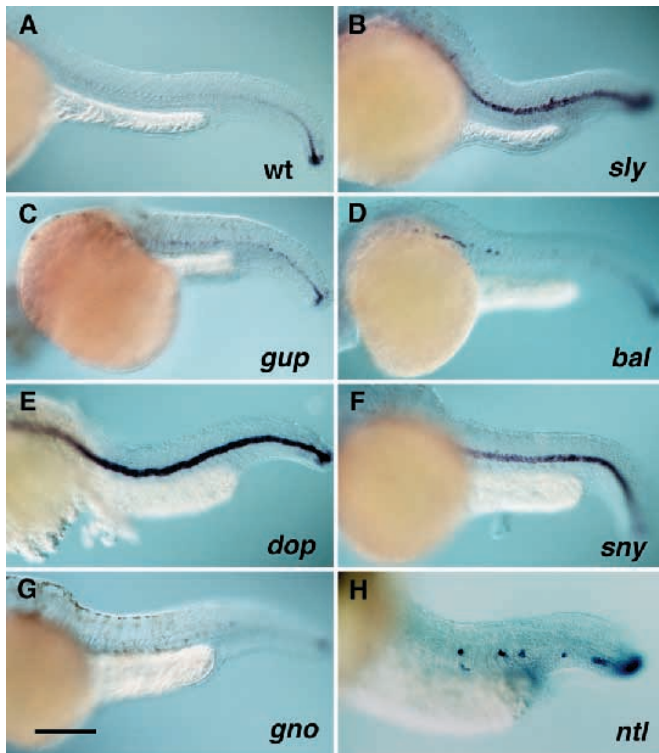
Fig. 4. *Brachyury* expression in mutants in the *sly*, *gup*, *bal*, *dop*, *sny*, *gno* and *ntl* loci. Shown are DIC micrographs of a 32 hpf (A) wild-type embryo, and (B) sly^{m466}, (C) gup^{m189}, (D) bal^{m190}, (E) dop^{m341}, (F) sny^{m456}, and (G) gno^{m622} mutant embryos and a 24 hpf (H) ntl^{m550} mutant embryo stained by in situ hybridization with anti-sense zebrafish *Brachyury* RNA. Scale bar, 250 µm.

are described elsewhere (Schier et al., 1996; Solnica-Krezel et al., 1996). Generally, mutants with abnormal notochords are reduced in body length (Figs 1, 6, 7). Each of the isolated mutations was tested for complementation with the other members of the group as well as with members of several other groups (Table 1). The 65 identified mutations define 29 complementation groups.

Chordamesoderm specification mutations (Group I)

Two genetic loci have been identified that appear to affect the formation of the chordamesoderm. These mutations act during gastrulation (Solnica-Krezel et al., 1996). The first locus is identified by the $bozozok^{m168}$ (boz^{m168}) mutation, which affects the formation of the entire axial mesoderm, i.e. both prechordal plate and chordamesoderm (Fig. 2). The most severely affected boz^{m168} mutants display a complete loss of both notochord and floor plate in combination with cyclopia. The failure of chordamesoderm to form can be observed during early segmentation stage by direct microscopic examination (Fig. 2A,B) as well as with a variety of molecular markers (see Solnica-Krezel et al., 1996). Although the notochord never forms in the most severe mutants (Fig. 2C,C′), the notochord is seen to form in the tail of some mutants (Fig. 2D) due to the variable expressivity of this mutation.

The only other locus affecting chordamesoderm specification is *floating head* (*flh*), which was previously recovered as a naturally occurring mutation (Talbot et al., 1995). We

recovered one new allele in the screen, flh^{m614}. Similar to mutants at the boz^{m168} locus, embryos mutant at the *flh* locus fail to form chordamesoderm properly and consequently fail to form a notochord.

Notochord differentiation mutations (Groups II, III and IV)

A relatively large group of 34 mutations in 8 genetic loci were found that appear to affect the transition from chordamesoderm to vacuolated notochord (Fig. 3). Based on specific features these 8 loci were further divided into three phenotypic groups. Group II mutations predominantly affect the notochord. Group III mutations affect both the notochord and the brain. Finally, Group IV mutations appear initially only to affect the notochord, but later in development the entire embryo degenerates. For 7 of the 8 loci, mutant embryos and wild-type siblings were stained with three probes marking several key steps in the development of the notochord, specifically, *Brachyury* (Fig. 4), *col2a1* (Fig. 5), and *shh* (Fig. 5). Additionally, to assay the ability of the mutant notochord to pattern the somites a monoclonal antibody against the Engrailed protein was used to mark the muscle pioneer cells at the horizontal myoseptum (Fig. 5).

Group II: mutations affecting the notochord

This group consists of two genetic loci and includes the previously described mutation in the zebrafish homologue of the mouse *Brachyury* gene called *no tail* (*ntl*), for which two new alleles were isolated (Halpern et al., 1993; Schulte-Merker et al., 1994). Mutants at the other locus $gnome^{m622}$ (gno^{m622}) are similar to *ntl* mutants. Mutations in each locus result in a markedly shortened body axis and the failure of the notochord to differentiate. Unlike *ntl* however, gno^{m622} mutants do not exhibit tail truncations. Additionally, whereas in *ntl* mutants Engrailed protein is not expressed in muscle pioneers (Halpern et al., 1993), in gno^{m622} mutants Engrailed is expressed in muscle pioneers, but at levels well below those of wild-type siblings (Fig. 5V). In gno^{m622} mutants both *Brachyury* and *col2a1* display patterns of expression that are virtually wild-type, with the exception that *col2a1* is occasionally ectopically expressed, perhaps due to anterior-posterior compression of the axis (Figs 4G, 5T). By contrast, mutants of the allele ntl^{m550} display an abnormal pattern of *Brachyury* expression (Fig. 4H), showing ectopic *Brachyury*-expressing cells along the axis including anterior regions where *Brachyury* expression has been already extinguished in wild-type siblings.

Group III: mutations affecting the notochord and brain

Group III (Table 1) consists of three loci each with a fairly large number of alleles. These three loci have strikingly similar mutant phenotypes including comparable brain defects, the failure of notochord to differentiate and a shortened body axis. The first locus is *sleepy* (*sly*). In mutants at this locus vacuolated notochord cells fail to differentiate (Fig. 3B). *Brachyury* expression in sly^{m466} mutants is wild type through at least the 20-somite stage (not shown). By 32 hpf, however, *Brachyury* staining becomes abnormal in mutant embryos (Fig. 4B). In some of the mutant embryos, *Brachyury* expression persists even in the most anterior portions of the chordamesoderm. In the remaining mutant embryos *Brachyury*-expressing cells are

found scattered along the axis. Furthermore, in all of the mutants *col2a1* expression persists at elevated levels at the mid-line along the entire axis (Fig. 5D). As with *ntl* and *flh*, the somites of *sly*[m466] mutants fail to form Engrailed-expressing muscle pioneers and subsequently fail to take on the normal chevron shape (Fig. 5F).
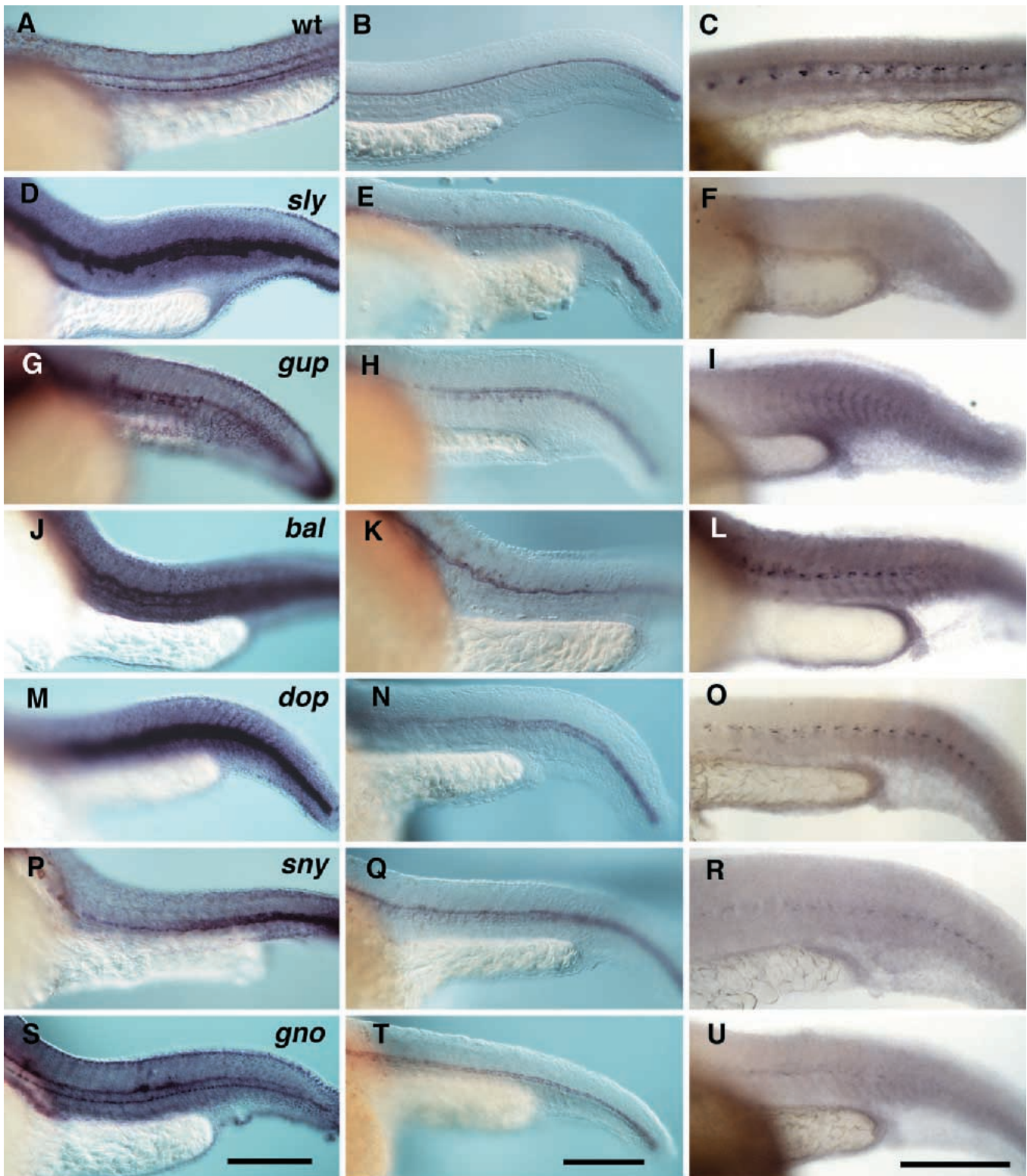

Fig. 5. *col2a1*, *shh*, and Engrailed expression in mutants in the *sly*, *gup*, *bal*, *dop*, *sny*, and *gno* loci. Shown are DIC micrographs of (A-C) wild-type embryos, and (D-F) *sly*[m466], (G-I) *gup*[m189], (J-L) *bal*[m190], (M-O) *dop*[m341], (P-R) *sny*[m456], and (S-U) *gno*[m622] mutant embryos stained by in situ hybridization with anti-sense zebrafish *col2a1* (A,D,G,J,M,P,S), *shh* (B,E,H,K,N,Q,T) RNA or with monoclonal anti-Engrailed antibody 4D9 (C,F,I,L,O,R,U). Embryos stained for *col2a1* are at 32 hpf and embryos stained for *shh* or Engrailed are at 24 hpf. Scale bars, 250 μm.

Embryos mutant in the *grumpy* (*gup*) locus have the same overall morphological appearance as *sly* mutants (Fig. 3C). Also, as in a subset of *sly* mutants, cells with persistent *Brachyury* expression are found scattered along the axis of *gup* mutants. In *gup^{m189}* mutants, however, *Brachyury* expression never persists throughout mutant notochord. The expression of *col2a1* in the notochord of *gup^{m189}* mutants appears normal except that a few ectopic *col2a1*-expressing cells are found along the axis (Fig. 5G). Expression of *col2a1* in the hypochord of *gup^{m189}* mutants is often disrupted (Fig. 5G). In addition, *gup^{m189}* fail to pattern somites properly. While Engrailed-expressing muscle pioneers can be found, they are few in number and exhibit very low levels of expression (Fig. 5I).

Mutants of the *bashful* (*bal*) locus have a morphologically abnormal notochord in the anterior region of the trunk, the defects are more pronounced in individuals carrying the strong alleles such as *bal^{m190}* (Fig. 3D). Mutants of the *bal* locus are similar to those of the *sly* and *gup* loci in that all three cause brain and eye defects (Schier et al., 1996), as well as defective anterior notochords. The alleles of *bal* are much more variable in their strength than alleles of *sly*. The weakest alleles of *bal*, such as *bal^{m268}*, tend to produce less pronounced notochord defects, presenting, for example, only a simple dysjunction in the anterior notochord. The strongest *bal* alleles, such as *bal^{m190}*, lack differentiated notochord only in the anterior part of the trunk. Both weak and strong alleles result in some brain defects (not shown). In these mutants there are also some ectopic *Brachyury*-expressing cells, primarily in the most anterior region of the notochord (Fig. 4D). Correlating with the *Brachyury* expression, *col2a1* is ectopically expressed in the anterior notochord of *bal^{m190}* mutants (Fig. 5J). The expression of *col2a1* in *bal^{m190}* mutant tails is, however, relatively wild-type although a bit compressed along the anterior-posterior axis (Fig. 5J). In the somites, Engrailed expression in anterior somites is relatively normal at 24 hpf (Fig. 5L). By 32 hpf the Engrailed expression in anterior somites is severely reduced, whereas in the tail, Engrailed expression remains normal.

Group IV: mutation affecting the notochord and causing degeneration

Three loci, *dopey* (*dop*), *sneezy^{m456}* (*sny^{m456}*), and *mikry^{m218}* (*mik^{m218}*) are related by a set of phenotypes, which at later stages of development includes degeneration throughout the embryo. Mutations at the *dop* or *sny* loci lead to the lack of a normally differentiated notochord at 24 hpf (Fig. 3E,F). The chordamesoderm continues to express both *Brachyury* and *col2a1* through 32 hpf of development (Figs 4E,F, 5M,Q). Engrailed expression in both *dop^{m341}* and *sny^{m456}* mutants is clearly reduced relative to wild-type siblings, both in terms of
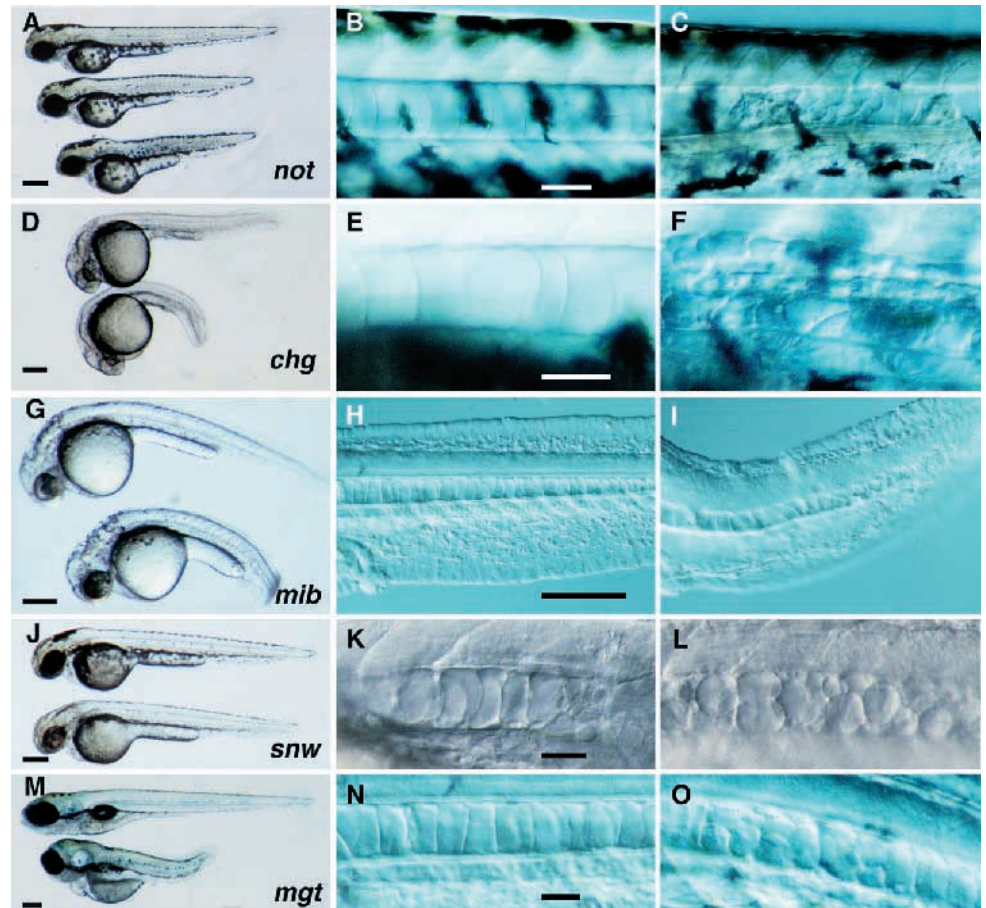

Fig. 6. Notochord phenotype of mutants in the *not, chg, mib, snw,* and *mgt* loci (A) The *not^{m128}* phenotype first becomes apparent at 48 hpf, manifest as regions of degeneration in the notochord (middle) or the notochord and muscle (lower). (B) Wild-type 48 hour notochord under DIC optics and (C) a *not^{m128}* mutant notochord displays abnormal cellular morphology and regions of degeneration. (D) The phenotype of *chg^{m275}* mutants becomes apparent by 24 hpf. By 48 hpf the notochord cellular morphology is abnormal throughout the axis. Shown is an anterior notochord from a 48 hpf wild-type embryo (E) and a corresponding region of a *chg^{m275}* mutant notochord (F). (G) Shown is a *mib^{m132}* mutant (lower) and a wild-type sibling (upper) at 24 hpf. (H) A 24 hpf wild-type tail and (I) *mib^{m132}* mutant tail show abnormal morphology of cells in the mutant notochord. The mutation *snw^{m454}* combines two phenotypes, regions of disrupted notochord with an overall failure to form melanophores properly. (J) In a 48 hpf *snw^{m454}* mutant (lower) the lack of melanophores is especially apparent on the yolk sac and in the head. The xanthophores and iridophores and the retinal pigmented epithelium are apparently unaffected. (K) A wild-type 28 hpf notochord displays the normal scalloped notochord cell morphology. (L) Regions of the notochord in *snw* mutants display an unusual phenotype in which rounded cells are present instead of the normally scalloped vacuolated notochord cells. (M) By 120 hpf *mgt^{m635}* mutant embryos (lower) are severly shorter than wild-type. Additionally, the mutants have abnormal craniofacial development including reduced branchial arch development. (N) A 32 hpf wild-type notochord and (O) a *mgt^{m635}* notochord with morphologically abnormal spherical cells. Scale bars, 250 μm (A,D,G,H,J,M); 50 μm (B,E,K,N).
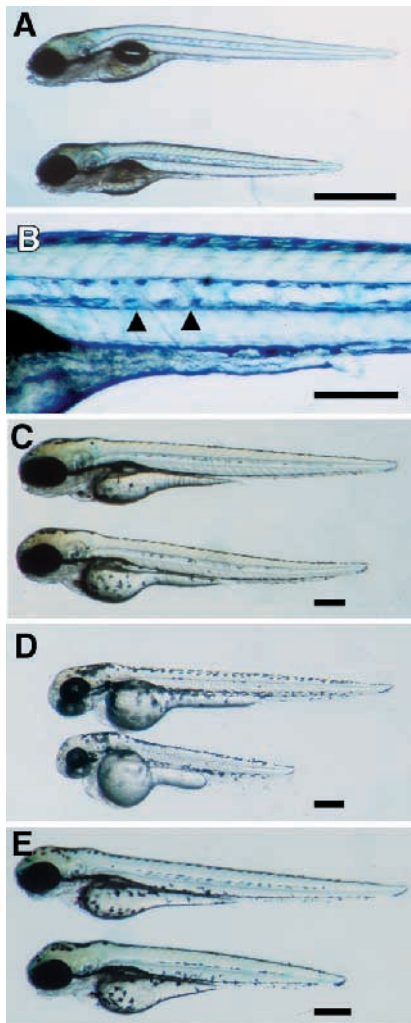
Fig. 7. Short axis and notochord phenotype of mutants in the *pro*, *sno*, *git*, and *drb* loci (A) Shown is a mutant (lower) at the *pro^m672* locus at 120 hpf with a wild-type sibling (upper). Scale bar = 1mm. (B) A higher magnification image of the *pro* mutants shows regions of disruption in the notochord (black arrowheads). (C) A mutant (lower) in the *sno^m563* locus at 72 hpf with a wild-type sibling (upper). (D) A mutant (lower) in the *git^m342* locus at 48 hpf with a wild-type sibling (upper). (E) A mutant (lower) in the *drb^m759* locus at 72 hpf with a wild-type sibling (upper). Scale bars, 250 μm (B-E).

the number of Engrailed-expressing cells and the level of Engrailed in each cell (Fig. 5P,S). The reduction, however, is not as extensive as that seen in *sly^m466* mutants, for example. The notochord of *mik^m218* mutants also fails to differentiate normally (Fig. 3H). Additionally, pigment formation in *dop*, *sny* and *mik* mutants is delayed (not shown). In mutants of *dop^m341* and *sny^m456* ventricles of the brain become slightly enlarged and by 60 hpf, the entire embryo becomes necrotic. Similar to *dop^m341* and *sny^m456*, *mik^m218* mutants manifest the combination of the notochord, pigmentation and early degeneration phenotypes with the exception that the onset of degeneration for *mik^m218* is at about 72 hpf.

By 24 hpf, *nototod^m128* (*not^m128*) mutants form a normal vacuolated notochord. Subsequently, regions of degeneration become apparent by 48 hpf (Fig. 6A-C). In a given cross about half of the mutants display degeneration of the notochord and the others show more general degeneration including both the notochord and somites. The *not* locus is partially non-complementing with the *ntl* locus. In crosses between *not^m128* and *ntl^m147* or *ntl^m550*, mutant embryos display the *not^m128* phenotype. The phenotype of transheterozygotes is weaker than *not^m128*/*not^m128* homozygotes and is not fully penetrant. The distinctiveness of the transheterozygous phenotype, i.e. notochord and somite degeneration has led us to treat *not* as a locus distinct from *ntl*.

Mutations affecting the maintenance of notochord structural integrity (Group V)

The mutants making up this group are related by the appearance of notochord defects only after the notochord cells have become vacuolated. In *snow white^m454* (*snw^m454*) mutants, notochord cells become vacuolated, but assume a spherical instead of the normal scalloped shape (Fig. 6J-L). Throughout the notochord normal-appearing notochord cells are interspersed with small round cells giving regions of the notochord a granular appearance. Additionally, melanophores of *snw^m454* do not form normally. By 5 dpf the overall length of the body of *snw* mutants is significantly reduced relative to that of wild-type siblings. Mutations at another locus, *mind bomb* (*mib*), lead to a similar spherical notochord cell morphology at 24 hpf (Fig. 6G-I), this often results in breaks in the notochord and a misshapen tail later in development. Additionally, these mutants overproduce several neuronal cell types and degenerate by 4 dpf (Schier et al., 1996). Mutations at the *changeling^m275* (*chg^m275*) locus cause a similar spherical notochord cell morphology at 48 hpf (Fig. 6D-F), which results in a bent tail at later stages. While initially fully penetrant, *chg^m275* displays reduced penetrance in heterozygous fish of generation F_3 or later. At 24 hpf *maggot* (*mgt*) mutant embryos show an abnormal curvature to the body and regions of abnormal spherical notochord cell morphology (Fig. 6O). At 48 hpf the notochord is thick in the anterior regions of the embryo and lacks the normal ventral flexure. The body is shorter and slightly curved, the head is of relatively normal shape (not shown). By 5 dpf mutant embryos are severely shorter than wild-type siblings, and possess an abnormally shaped head with underdeveloped branchial arches, and malformed ear (Neuhauss et al., 1996) (Fig. 6M).

Mutations at other loci within this group, *gitolo^m342* (*git^m342*), *drobny^m759* (*drb^m759*), *snorri* (*sno*), and *proteus^m642* (*pro^m642*), cause focal notochord disruptions (Fig. 7). In disrupted regions notochord cells take on an abnormal appearance, which may be degeneration, at a relatively late stage of development. A mutation at the *proteus^m642* (*pro^m642*) locus produces such disruptions at 4 dpf (Fig. 7B).

Mutations that produce folded notochords (Group VI)

The two mutations *gulliver^m208* (*gul^m208*) and *leviathan^m531* (*lev^m531*) result in a folded notochord phenotype at 24 hpf (Fig. 8A,B). In *lev* mutants the notochord is folded both laterally and dorsoventrally (Fig. 8F,F′). The folding in *gul*, by contrast, is in a dorsal-ventral orientation (Fig. 8A). While in *gul^m208* the notochord straightens out by 3 dpf (Fig. 8C), in *lev^m531*, the folded notochord phenotype becomes more severe over time. Additionally *gul^m208* has a brain phenotype leading to a

severely reduced head size by 5 dpf by which time the notochord is elongated, producing an overall body length greater than that of wild-type siblings (Fig. 8C). The *lev^m531* allele has a weak-dominant character with a penetrance of about 10% when crossed with wild-type fish.

Mutations in the two loci, *trilobite* (*tri*) and *knypek* (*kny*) lead to a reduction in convergence and extension during gastrulation (Solnica-Krezel et al., 1996). They also cause severe folding of the notochord in the tail by 5 dpf (Fig. 8D,E).

DISCUSSION

Mutations affecting notochord formation

In a screen for recessive zygotic-effect mutations affecting zebrafish embryogenesis we found 65 mutations that affect the development of the notochord. Complementation testing indicates that there are 29 distinct genetic loci making up the notochord mutations. The fact that the notochord passes through several distinguishable stages allows us to order the genetic loci in a pathway controlling notochord morphogenesis. Starting from the beginning of the pathway (Fig. 9) we found two loci, *flh* and *boz* that appear to control either the formation or the maintenance of chordamesoderm (Talbot et al., 1995). A relatively large number of loci are apparently involved in the normal transition of chordamesoderm to vacuolated notochord (Fig. 10, 'early notochord'). These mutations may, in effect, arrest the notochord at specific stages of its development. This notion is suggested by the fact that several markers are persistently expressed in mutants. Although it is difficult to determine the relative order of the 'notochord differentiation' loci, it is possible to group them according to relatedness of the phenotypes they produce. Hence, *ntl* and *gno* are grouped because they affect the notochord predominantly. The loci *sly, gup,* and *bal* are grouped because they produce a combination of notochord and brain phenotypes (Schier et al., 1996) and finally *dop, sny,* and *mik* are grouped together because they lead to degeneration of the whole embryo. A third group of 9 loci appear to control later stages of notochord differentiation (Fig. 9, 'late notochord'). They all exhibit their mutant phenotype after the notochord has become vacuolated. Mutations at the first 4 loci, *snw, mib, mgt,* and *chg* produce notochord cells with an abnormal spherical morphology. Mutants at the *not* locus develop an abnormal notochord cell morphology by 48 hpf, possibly reflecting cell death. Degeneration becomes more generalized in *not* mutants affecting also the muscles. Finally, for the last 4 loci, *git, drb, sno* and *pro*, mutants

exhibit focal disruptions in the notochord integrity. For mutants of the 'late notochord' loci, the failure of differentiated notochord cells to maintain their normal scalloped morphology may be the result of failure in a variety of different physiological pathways. One possiblity is that some or all of the notochord cells in these mutants are destined to die, in which case the gene may serve a maintenance function for cell survival. For example, these genes may be involved in a trophic response pathway. Alternatively, these genes may be involved in the formation of the notochord sheath. In zebrafish, the notochord is made up of a core of vacuolated cells surrounded by a sheath of cells or extracellular matrix (Kimmel et al., 1995). If the sheath were not to form or to break down, the structural integrity of the notochord may be compromised, resulting in the degeneration or loss of vacuolated notochord cells. The expression of these late-acting genes may be controlled by genes acting earlier in the pathway (Fig. 10), and one aspect of control may be the decision to form sheath. The composition of the sheath needs to be investigated in this context.

Mutations affecting notochord shape

The loci controlling notochord shape are difficult to place in the pathway of notochord development. Some of these loci may not function directly in the notochord, but may instead control more general aspects of cell movement during gastrulation, or may result from inappropriate interactions with the surrounding tissues. The mutations at the *tri* and *kny* loci, for example, clearly reduce convergence and extension during gastrulation. Given that the notochord is vacuolated normally in these mutants and is only affected in the tail, these loci may
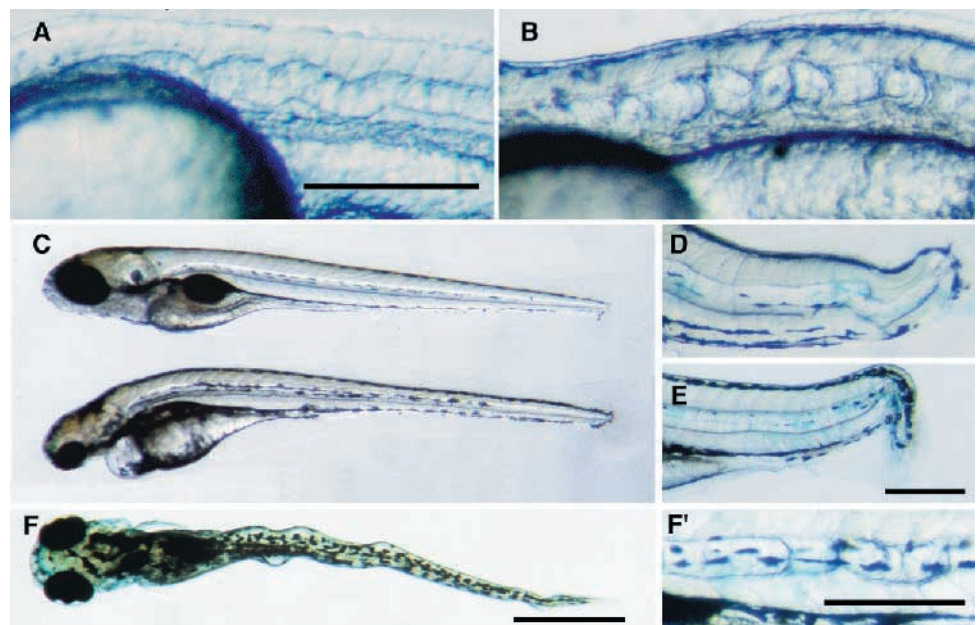

Fig. 8. Notochord shape phenotype of mutants in the *gul, lev, bup, tri* and *kny* loci A wavy notochord phenotype by 28 hpf characterizes the two mutations *gul^m208* (A) and *lev^m531* (B). (C) By 72 hpf *gul^m208* mutants have a straight notochord and a severe head malformation (bottom). (F, F′) By contrast, by 96 hpf in *lev^m531* mutants the wavy notochord phenotype is exacerbated and shows both lateral (F) and dorsal-ventral flexures (F′). The gastrulation mutations *tri^m144* (D) and *kny^m119* (E) exhibit a folded notochord phenotype only in the tail at 72 hpf. Scale bars, 250 μm (A,E, F′) and 1 mm (A,F).
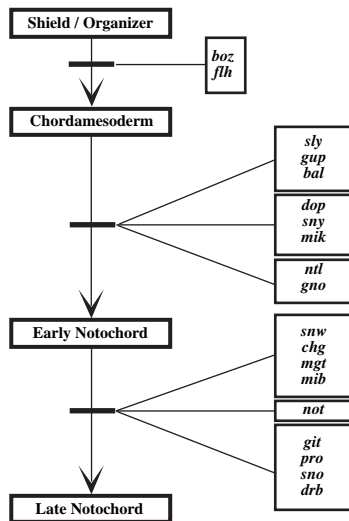
Fig. 9. Model of notochord formation and maintenance: A phenotypic pathway. Tissues at various stages of development are represented by the horizontal boxes. Heavy black arrows between tissues represent a progenitor-product relationship between the tissues. Mutations thought to act in a given process are listed in boxes with thin lines connecting them to heavy horizontal bars that, in turn, denote the place or developmental stage at which the associated mutations seem to act primarily.

not primarily control notochord shape but may primarily affect morphogenesis of the tail (Solnica-Krezel et al., 1996). The severely shortened tail in *tri* and *kny* mutants may not provide enough space for the notochord, which unable to elongate, is forced to fold. Conversely, given that these loci control aspects of gastrulation movements, including convergence and extension of chordamesoderm, the effects on notochord shape may be the result of a failure of convergence or extension in the chordamesoderm at an earlier time in development.

Role of notochord in embryonic patterning
Floor plate induction

Steps in the pathway of differentiation may also be reflected in the signaling activity of the notochord. There are several clear examples of notochord signaling activity important to the patterning of trunk structures. Using notochord transplantation assays and in vitro explants several groups have shown that notochord can induce floor plate to form (Placzek et al., 1993; van Straaten et al., 1985, 1988; Yamada et al., 1993). The induction of the floor plate is a contact-dependent interaction which is mimicked by Sonic hedgehog protein (Roelink et al., 1994).

Mutations that lead to defects in floor plate formation fall into two classes. When the chordamesoderm is eliminated, as in *boz* and *flh* mutants the floor plate does not form or is severely reduced (Solnica-Krezel et al., 1996; Talbot et al., 1995). By contrast, mutants of the 'notochord differentiation' loci all form a floor plate as indicated by the expression of *col2a1* (Fig. 5) and *shh* (Fig. 5). Likewise, for mutants of the 'notochord maintenance' class the floor plate forms normally. The other class of mutations that leads to floor plate defects includes the *cyc*, *oep* and *unf* loci. Mutants at these loci display reductions in the number of floor plate cells, but have relatively mild notochord defects. For example, mutants of the *cyc* locus express *col2a1* in the notochord for an abnormally long time (Yan et al., 1995). Additionally, *cyc* mutants have a reduced prechordal plate as measured both by the number of hatching gland cells produced and the expression of *goosecoid* (Thisse et al., 1994). The loss of floor plate cells in *cyc* may therefore be a consequence of the failure to specify the axial mesoderm properly. Mutations in the *unf* locus lead to a reduction in the number of floor plate cells and to a mild cyclopean phenotype, similar to weak allele mutants of the *cyc* locus, such as cyc^{m101} (Schier et al., 1996).

The induction of motoneurons is related to the induction of floor plate. Both the notochord and the floor plate are capable of inducing motoneurons to differentiate (Yamada et al., 1993). Additionally, *shh* may mediate motoneuron induction (Roelink et al., 1995). It will be of interest to determine if there are any motoneuron induction defects among mutants of the notochord differentiation loci. The brain phenotypes of the *sly, gup* and *bal* mutants suggest a reduction in the amount of ventral CNS tissue (Schier et al., 1996). If the CNS phenotype is a secondary consequence of abnormal notochord differentiation, reductions in neuron number may reflect the loss of one ventral specification signal source. The floor plate of these mutants is present, but without differentiated notochord there may not be enough signal to specify the ventral spinal cord completely. Alternatively, a qualitatively different signal may be present in the mutants causing the ventral spinal cord to be specified in an inappropriate fashion. A careful qualitative analysis of ventral spinal cord specification and quantification of motoneuron number may reveal a change in the quality or amount of ventral signal in notochord differentiation mutants. Such analyses remain to be performed.

Somite patterning

There have been several reports of notochord and/or neural tube specification of somitic cell fate. Transplantation of notochord or floor plate to abnormal dorsolateral positions results in the specification of sclerotomal fate at the expense of dermomyotome (Pourquie et al., 1993). Moreover, in explants of caudal somites and segmental plate mesoderm, both the notochord and neural tube were able to specify myogenic fates in unspecified somitic tissue (Buffinger and Stockdale, 1994). Among the mutant embryos lacking chevron shaped somites, muscle pioneers, as detected by staining with a monoclonal anti-Engrailed antibody, are also disrupted. This correlation was previously reported for *ntl* (Halpern et al., 1993) and is also true of *flh*, which acts much earlier in the notochord differentiation pathway. Mutations at the *sly, bal, gup, gno^{m622}, dop,* and sny^{m456} loci lead to improperly patterned somitic tissue. Taken together these observations suggest two steps in the control of Engrailed expression in muscle pioneers. The first step is a notochord- or chordamesoderm-derived signal specifying Engrailed expression in the pioneers (Halpern et al., 1993). The loci *flh, ntl* and *sly* are important in controlling this step since Engrailed is not expressed in the somites of mutants in these loci at 24 hpf. The second step is a notochord-derived signal needed for the maintained expression of Engrailed in muscle pioneers. This second step may be controlled by the *gup, bal, dop, sny* and *gno* loci (Fig. 10). A similar two-step process under control of notochord-derived signals has been described for the

expression of *Pax-1* in the forming sclerotome of mouse notochord mutants (Dietrich et al., 1993). Clearly a more detailed analysis of expression patterns of a variety of ventral and cell-type specific markers is required for these mutations. Additionally, it would be of interest to determine if the 'adaxial' region, which is the paraxial mesoderm immediately apposing the notochord, is properly specified in the mutants (Thisse et al., 1993). Such analyses will be important to dissect the signalling capacity of the notochord.

Patterning of other tissues

Several other patterning roles of the notochord remain to be examined in these mutants. For example, in vivo notochord extirpation and neural tube inversion studies indicate that the notochord and/or floor plate is necessary for the formation of sympathoadrenal progenitors in the paravertebral ganglia (Stern et al., 1991). Since sympathoadrenal progenitors form at a fairly late stage, 5-7 dpf in zebrafish (Paul Henion, personal communcation), it may be possible to define additional steps in notochord maturation pathway based on the ability of mutant notochord to signal sympathoadrenal formation. There is also some indication of relevant interactions between the notochord and the developing gut (Wiertz-Hoessels et al., 1987). Additionally, the notochord has been implicated in the patterning of left-right asymmetry of the heart tube (Danos and Yost, 1995). It will be important for us to examine in detail the specification of all somitic derivatives, of sympathetic ganglia, gut and other tissues in addition to the neurectoderm. Specification of the different cell types may be controlled by different notochord-derived signals and those signals may be differentially affected by the notochord mutations.

Pleiotropy of mutations affecting notochord development

Most of the mutations presented here affect tissues other than the notochord. Two categories are prevalent. The first category includes the Group III loci, *sly*, *bal*, and *gup*. On the one hand, the brain defects of these mutants may reflect the loss of signalling activity from the notochord and/or the prechordal plate. Alternatively, these genes may be utilized independently in each tissue. Similarly, all of the mutations affecting patterning of the somites may reflect a requirement for wild-type gene activity in both the notochord and somites. The second category includes the mutations that lead also to general degeneration of the embryo, the Group IV loci. It is possible that these mutations control some general aspect of cell-cycle control or growth and that the notochord phenotype is coincident. Contrary to this idea, by 24 hpf development of other tissues appears to proceed normally in these mutants. For example, the expression of Engrailed at the midbrain/hindbrain boundary is normal in mutants possessing undifferentiated notochords. Additionally, many other mutations with demonstrable developmental delays or degeneration possess morphologically normal notochords (Abdelilah et al., 1996). Moreover, preliminary staining for DNA fragmentation in *dop*^*m341*^ mutants indicates that cell death is occurring selectively in the notochord at 24 hpf (D. L. S., unpublished observations). By 32 hpf, however, the general delay in these mutants is obviated by a reduction in the amount of pigmentation.

In summary, of the zygotic-lethal mutations affecting embryogenesis identified in our screen, a group of 29 genetic loci are involved in the formation and maintenance of the notochord. The mutations will be valuable for studies of vertebrate development in two general ways. First, the mutations will provide access to key genes controlling the formation and differentiation of the notochord. Second, the mutations are useful tools for dissecting a host of cellular interactions underlying pattern formation in the embryo.

REFERENCES

Abdelilah, S., Mountcastle-Shah, E., Harvey, M., Solnica-Krezel, L., Schier, A. F., Stemple, D. L., Malicki, J., Neuhauss, S. C. F., Zwartkruis, F., Stainier, D. Y. R., Rangini, Z. and Driever, W. (1996). Mutations affecting neural survival in the zebrafish, *Danio rerio*. *Development* **123**, 217-227.

Adams, D. S., Keller, R. and Koehl, M. A. (1990). The mechanics of notochord elongation, straightening and stiffening in the embryo of Xenopus laevis. *Development* **110**, 115-130.

Ang, S. L. and Rossant, J. (1994). HNF-3 beta is essential for node and notochord formation in mouse development. *Cell* **78**, 561-574.

Berry, R. J. (1960). Genetical studies on the skeleton of the mouse. XXVI. Pintail. *Genet. Res.* **1**, 439-451.

Bober, E., Brand-Saberi, B., Ebensperger, C., Wilting, J., Balling, R., Paterson B, M., Arnold, H. H. and Christ, B. (1994). Initial steps of myogenesis in somites are independent of influence from axial structures. *Development* **120**, 3073-3082.

Bovolenta, P. and Dodd, J. (1991). Perturbation of neuronal differentiation and axon guidance in the spinal cord of mouse embryos lacking a floor plate: Analysis of Danforth's short-tail mutation. *Development* **113,** 625-639.

Buffinger, N. and Stockdale, F. E. (1994). Myogenic specification in somites: induction by axial structures. *Development* **120**, 1443-1452.

Christ, B., Brant-Saberi, B., Grim, M. and Wilting, J. (1992). Local signalling in dermomyotomal cell type specification. *Anat. Embryol.* **186**, 505-510.

Danos, M. C. and Yost, H. J. (1995). Linkage of cardiac left-right asymmetry and dorsal-anterior development in *Xenopus*. *Development* **121**, 1467-1474.

Dietrich, S., Schubert, F. R. and Gruss, P. (1993). Altered *Pax* gene expression in murine notochordal mutants: the notochord is required to initiate and maintain ventral identity in the somite. *Mech. Dev.* **44**, 189-207.

Driever, W., Solnica-Krezel, L., Schier, A. F., Neuhauss, S. C. F., Malicki, J., Stemple, D. L., Stainier, D. Y. R., Zwartkruis, F., Abdelilah, S., Rangini, Z., Belak, J. and Boggs, C. (1996). A genetic screen for mutations affecting embryogenesis in zebrafish. *Development* **123**, 37-46.

Fan, C. M., Porter, J. A., Chiang, C., Chang, D. T., Beachy, P. A. and Tessier-Lavigne, M. (1995). Long-range sclerotome induction by sonic hedgehog: direct role of the amino-terminal cleavage product and modulation by the cyclic AMP signaling pathway. *Cell* **81**, 457-465.

Fan, C. M. and Tessier-Lavigne, M. (1994). Patterning of mammalian somites by surface ectoderm and notochord: evidence for sclerotome induction by a hedgehog homolog. *Cell* **79**, 1175-1186.

George, E. L., George-Labouesse, E. N., Patel-King, R. S., Rayburn, H. and Hynes, R. O. (1993). Defects in mesoderm, neural tube and vascular development in mouse embryos lacking fibronectin. *Development* **119**, 1079-1091.

Goulding, M. D., Lumsden, A. and Gruss, P. (1993). Signals from the

notochord and floor plate regulate the region-specific expression of two Pax genes in the developing spinal cord. *Development* **117**, 1001-1016.

Halpern, M. E., Ho, R. K., Walker, C. and Kimmel, C. B. (1993). Induction of muscle pioneers and floor plate is distinguished by the zebrafish no tail mutation. *Cell* **75**, 99-111.

Hatta, K., Bremiller, R., Westerfield, M. and Kimmel, C. B. (1991a). Diversity of expression of engrailed-like antigens in zebrafish. *Development* **112**, 821-832.

Hatta, K., Kimmel, C. B., Ho, R. K. and Walker, C. (1991b). The cyclops mutation blocks specification of the floor plate of the zebrafish central nervous system. *Nature* **350**, 339-341.

Herrmann, B. G., Labeit, S., A., P., King, T. R. and Lerach, H. (1990). Cloning of the T gene required in mesoderm formation the mouse. *Nature* **343**, 617-622.

Ho, R. K. (1992). Axis formation in the embryo of the zebrafish, *Brachydanio rerio*. *Sem. Dev. Biol.* **3**, 53-64.

Johnson, R. L., Laufer, E., Riddle, R. D. and Tabin, C. (1994a). Ectopic expression of Sonic hedgehog alters dorsal-ventral patterning of somites. *Cell* **79**, 1165-1173.

Johnson, S. L., Midson, C. N., Ballinger, E. W. and Postlethwait, J. H. (1994b). Identification of RAPD primers that reveal extensive polymorphisms between laboratory strains of zebrafish. *Genomics* **19**, 152-156.

Jowett, T. and Lettice, L. (1994). Whole-mount in situ hybridizations on zebrafish embryos using a mixture of digoxigenin- and fluorescein-labelled probes. *Trends Genet.* **10**, 73-74.

Kimmel, C. B., Ballard, W. M., Kimmel, S. R., Ullmann, B. and Schilling, T. F. (1995). Stages of embryonic development of the zebrafish. *Dev. Dyn.* **203**, 253-310.

Knapik, E. W., Goodman, A., Atkinson, O. S., Roberts, C. T., Shiozawa, M., Sim, C. U., Weksler-Zangen, S., Trolliet, M. R., Futrell, C., Innes, B. A., Koike, G., McLaughlin, M. G., Pierre, L., Simon, J. S., Vilallonga, E., Roy, M., Chiang, P.-W., Fishman, M. C., Driever, W. and Jacob, H. J. (1996). A reference cross DNA panel for zebrafish (*Danio rerio*) anchored with simple sequence length polymorphisms. *Development* **123**, 451-460.

Krauss, S., Concordet, J. -P. and Ingham, P. W. (1993). A functionally conservered homolog of the drosophila segment polarity gene *hh* is expressed in tissues with polarizing activity in zebrafish embryos. *Cell* **75**, 1431-1444.

Lyons, K. M., Hogan, B. L. M. and Robertson, E. J. (1995). Colocalization of BMP 7 and BMP 2 RNAs suggests that these factors cooperatively mediate tissue interactions during murine development. *Mech. Dev.* **50**, 71-83.

Mullins, M. C. and Nüsslein-Volhard, C. (1993). Mutational approaches to studying embryonic pattern formation in the zebrafish. *Curr. Op. Genet. Dev.* **3**, 648-654.

Neuhauss, S. C. F., Solnica-Krezel, L., Schier, A. F., Zwartkruis, F., Stemple, D. L., Malicki, J., Abdelilah, S., Stainier, D. Y. R. and Driever, W. (1996). Mutations affecting craniofacial development in zebrafish. *Development* **123**, 357-367.

Oppenheimer, J. M. (1936). Transplantation experiments on developing teleosts (Fundulus and Perca). *J. Exp. Zool.* **72**, 247-269.

Oxtoby, E. and Jowett, T. (1993). Cloning of the zebrafish krox-20 gene (krx-20) and its expression during hindbrain development. *Nucl. Acids Res.* **21**, 1087-1095.

Paavola, L. G., Wilson, D. B. and Center, E. M. (1980). Histochemistry of the developing notochord, perichordal sheath and vertebrae in Danforth's short-tail (Sd) and normal C57BL/6 mice. *J. Embryol. Exp. Morphol.* **55**, 227-245.

Phelps, D. E. and Dressler, G. R. (1993). Aberrant expression of Pax-2 in Danforth's short tail (Sd) mice. *Dev. Biol.* **157**, 251-258.

Placzek, M., Jessell, T. M. and Dodd, J. (1993). Induction of floor plate differentiation by contact-dependent, homeogenetic signals. *Development* **117**, 205-18.

Pourquie, O., Coltey, M., Teillet, M. A., Ordahl, C. and Le Douarin, N. (1993). Control of dorsoventral patterning of somitic derivatives by notochord and floor plate. *Proc. Natl. Acad. Sci. USA* **90**, 5242-6.

Roelink, H., Augsburger, A., Heemskerk, J., Korzh, V., Norlin, S., Ruiz i

Altaba, A., Tanabe, Y., Placzek, M., Edlund, T., Jessell, T. M. and Dodd, J. (1994). Floor plate and motor neuron induction by vhh-1, a vertebrate homolog of hedgehog expressed by the notochord. *Cell* **76**, 761-775.

Roelink, H., Porter, J. A., Chiang, C., Tanabe, Y., Chang, D. T., Beachy, P. A. and Jessell, T. M. (1995). Floor plate and motor neuron induction by different concentrations of the amino-terminal cleavage product of sonic hedgehog autoproteolysis. *Cell* **81**, 445-455.

Rong, P. M., Teillet, M. A., Ziller, C. and Le Douarin, N. M. (1992). The neural tube/notochord complex is necessary for vertebral but not limb and body wall striated muscle differentiation. *Development* **115**, 657-672.

Schier, A. F., Neuhauss, S. C. F., Harvey, M., Malicki, J., Solnica-Krezel, L., Stainier, D. Y. R., Zwartkruis, F., Abdelilah, S., Stemple, D. L., Rangini, Z., Yang, H. and Driever, W. (1996). Mutations affecting the development of the embryonic zebrafish brain. *Development* **123**, 165-178.

Schulte-Merker, S., Ho, R. K., Herrmann, B. G. and Nüsslein-Volhard, C. (1992). The protein product of the zebrafish homologue of the mouse T gene is expressed in nuclei of the germ ring and the notochord of the early embryo. *Development* **116**, 1021-1032.

Schulte-Merker, S., van Eeden, F. J. M., Halpern, M. E., Kimmel, C. B. and Nüsslein-Volhard, C. (1994). *no tail (ntl)* is the zebrafish homologue of the mouse T (*Brachyury*) gene. *Development* **120**, 1009-1015.

Solnica-Krezel, L., Schier, A. F. and Driever, W. (1994). Efficient recovery of ENU-induced mutations from the zebrafish germline. *Genetics* **136**, 1401-1420.

Solnica-Krezel, L., Stemple, D. L., Mountcastle-Shah, E., Rangini, Z., Neuhauss, S. C. F., Malicki, J., Schier, A. F., Stainier, D. Y. R., Zwartkruis, F., Abdelilah, S. and Driever, W. (1996). Mutations affecting cell fates and cellular rearrangements during gastrulation in zebrafish. *Development* **123**, 67-80.

Spemann, H. (1938). *Embryonic Development and Induction*. New Haven, CT: Yale University Press.

Stern, C. D., Artinger, K. B. and Bronner-Fraser, M. (1991). Tissue interactions affecting the migration and differentiation of neural crest cells in the chick embryo. *Development* **113**, 207-216.

Talbot, W. S., Trevarrow, B., Halpern, M. E., Melby, A. E., Farr, G., Postlethwait, J. H., Jowett, T., Kimmel, C. B., Kimmelmann, D. (1995). A homeobox gene essential for zebrafish notochord development. *Nature* **378**, 150-157.

Theiler, K. (1959). Anatomy and development of the 'truncate' (Boneless) mutation in the mouse. *Am. J. Anat.* **104**, 319-343.

Thisse, C., Thisse, B., Halpern, M. E. and Postlethwait, J. H. (1994). *goosecoid* expression in neurectoderm and mesendoderm is disrupted in zebrafish cyclops gastrulas. *Dev. Biol.* **164**, 420-429.

Thisse, C., Thisse, B., Schilling, T. F. and Postlethwait, J. H. (1993). Structure of the zebrafish *snail1* gene and its expression in wild-type, *spadetail*, and *no tail* mutant embryos. *Development* **119**, 1203-1215.

van Straaten, H. W., Hekking, J. W., Thors, F., Wiertz-Hoessels, E. L. and Drukker, J. (1985). Induction of an additional floor plate in the neural tube. *Acta Morph. Neer. Scand.* **23**, 91-97.

van Straaten, H. W., Hekking, J. W., Wiertz-Hoessels, E. J., Thors, F. and Drukker, J. (1988). Effect of the notochord on the differentiation of a floor plate area in the neural tube of the chick embryo. *Anat. Embryol.* **177**, 317-24.

Weinstein, D. C., Ruiz i Altaba, A., Chen, W. S., Hoodless, P., Prezioso, V. R., Jessell, T. M. and Darnell, J. (1994). The winged-helix transcription factor HNF-3 beta is required for notochord development in the mouse embryo. *Cell* **78**, 575-588.

Wiertz-Hoessels, E. L., Hara, K., Hekking, J. W., van Straaten, H. W., Thors, F. and Drukker, J. (1987). Differentiation of gut endoderm in dependence of the notochord. *Anat. Emb.* **176**, 337-343.

Yamada, T., Pfaff, S. L., Edlund, T. and Jessell, T. M. (1993). Control of cell pattern in the neural tube: motor neuron induction by diffusible factors from notochord and floor plate. *Cell* **73**, 673-686.

Yan, Y.-L., Hatta, K., Riggleman, B. and Postlethwait, J. H. (1995). Expression of a type II collagen gene in the zebrafish embryonic axis. *Dev. Dyn.* **203**, 363-376.